Melting of Three-Sublattice Order in Easy-Axis Antiferromagnets on Triangular and Kagome Lattices

Kedar Damle
Tata Institute of Fundamental Research, 1 Homi Bhabha Road, Mumbai 400005, India
(Received 4 October 2014; published 16 September 2015)

When the constituent spins have an energetic preference to lie along an easy axis, triangular and kagome lattice antiferromagnets often develop long-range order that distinguishes the three sublattices of the underlying triangular Bravais lattice. In zero magnetic field, this three-sublattice order melts *either* in a two-step manner, i.e., via an intermediate phase with power-law three-sublattice order controlled by a temperature-dependent exponent $\eta(T) \in (\frac{1}{9}, \frac{1}{4})$, *or* via a transition in the three-state Potts universality class. Here, I predict that the uniform susceptibility to a small easy-axis field B diverges as $\chi(B) \sim |B|^{-[(4-18\eta)/(4-9\eta)]}$ in a large part of the intermediate power-law ordered phase [corresponding to $\eta(T) \in (\frac{1}{9}, \frac{2}{9})$], providing an easy-to-measure thermodynamic signature of two-step melting. I also show that these two melting scenarios can be generically connected via an intervening multicritical point and obtain numerical estimates of multicritical exponents.

DOI: 10.1103/PhysRevLett.115.127204 PACS numbers: 75.10.Jm

In frustrated antiferromagnets [1,2], magnetic ions (spins) form a lattice whose geometry causes the dominant antiferromagnetic interactions between neighbors to compete with each other. This allows weaker further-neighbor interactions or quantum fluctuations to select complex patterns of spin order at low temperature. Models of frustrated easy-axis antiferromagnets [3,4], in which spins can lower energy by orienting along a fixed axis, provide interesting examples of this behavior.

Such models are also relevant in other experimental contexts. For instance, the low-temperature behavior of monolayers of adsorbed gases on substrates with triangular symmetry [5–11] has been modeled [12] in terms of a triangular lattice of Ising spins $\sigma^z_{\vec{R}} = \pm 1$ ($\hat{z}$ components of spin-half moments $\vec{S}_{\vec{R}} = \vec{\sigma}_{\vec{R}}/2$) with antiferromagnetic Ising interactions $J\sigma^z_{\vec{R}}\sigma^z_{\vec{R}'}$ between nearest neighbors [13,14] and weak ferromagnetic Ising interactions between further neighbors. More recently, the magnetic properties of honeycomb networks [15–18] of magnetic wires (dubbed artificial kagome ice) have been analyzed [19–21] in terms of a similar Ising model on the kagome lattice [22]. In both examples, further-neighbor couplings cause the Ising spins to develop ferrimagnetic three-sublattice order at low temperature, i.e., freeze into a pattern which distinguishes the three sublattices of the underlying triangular Bravais lattice and gives rise to a small net moment along the easy axis.

Several other easy-axis spin systems on triangular and kagome lattices exhibit ferrimagnetic three-sublattice order [23–34] or closely related antiferromagnetic (no net easy-axis moment) three-sublattice order [35]. In zero field ($B = 0$) along the easy axis, a Ginzburg-Landau theory [36–38] for the three-sublattice order parameter predicts that this ordering transition is described by a sixfold anisotropic effective model of ferromagnetically coupled XY spins [39] or, equivalently, by a generalized six-state clock model [40–43]. Rather unusually, such six-state clock models have multiple generic possibilities for continuous transitions: order is lost *either* via a two-step melting transition, with an intermediate phase characterized by power-law order [39], *or* via a sequence of two distinct transitions, one of which is in the three-state Potts universality class and the other in the Ising universality class [40,41]. Perhaps motivated by this, the melting of three-sublattice order has been studied in a variety of triangular and kagome lattice systems for over three decades now. In some examples [12,23–26,35], three-sublattice order is known to melt in a two-step manner via a sizeable intermediate phase with power-law three-sublattice order controlled by a temperature-dependent exponent $\eta(T) \in (\frac{1}{9}, \frac{1}{4})$. In other examples with *ferrimagnetic* three-sublattice order, this order is lost via a three-state Potts transition, while residual *ferromagnetism* is lost via an Ising transition [19–21].

In this Letter, I analyze the melting of three-sublattice order in easy-axis antiferromagnets on triangular and kagome lattices using a new coarse-grained description that explicitly keeps track of the uniform easy-axis magnetization mode whose fluctuations are coupled to fluctuations of the three-sublattice order parameter. Using this description, which goes beyond the standard Ginzburg-Landau theory, I demonstrate that these two very different melting processes can be generically connected via an intervening multicritical point $\mathcal{M}$ (Fig. 2) with central charge [44] $c_{\mathcal{M}} \in (1, \frac{3}{2})$. Although the generalized six-state clock model correctly captures other generic ways [40,41] in which these two very different melting processes can be separated from each other in the phase diagram of such

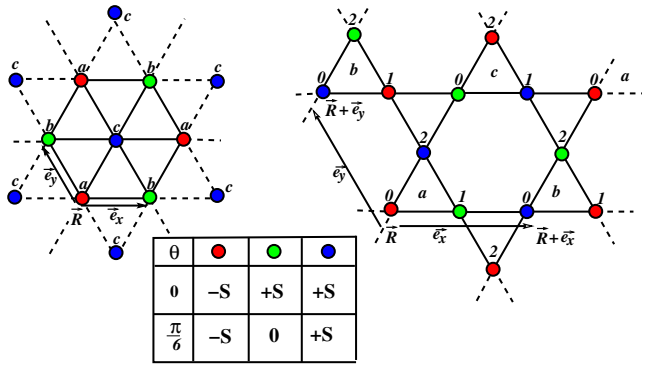

FIG. 1 (color online). Color-coded symbols on sites give the value of $\langle S^z_{\vec{r}}\rangle$ in the presence of ferrimagnetic ($\theta = 0$) or antiferromagnetic ($\theta = \pi/6$) three-sublattice order in spin-S triangular (kagome) lattice easy-axis antiferromagnets. These ordering patterns distinguish between the three sublattices of the underlying Bravais lattice of sites (up-pointing triangles).

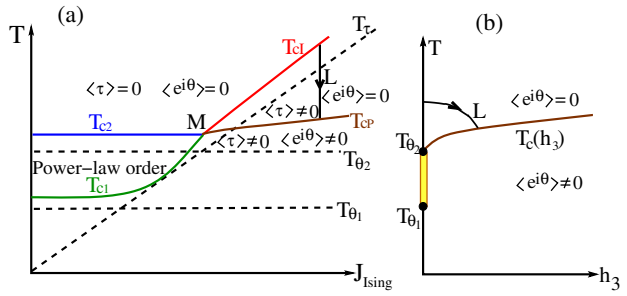

FIG. 2 (color online). (a) Predicted structure of the $T - J_{\rm Ising}$ phase diagram of $H_{\rm eff}$ for $h = 0$ and fixed J_{xy} and $J_{\theta\tau}$. Phase boundaries of $H_{\rm eff}$ are depicted by color-coded solid lines, while those of $H_{\rm Ising}$ and $H_{\rm xy}$ are displayed as dashed lines. (b) Known $T - h_3$ phase diagram of $H_{xy} - h_3\sum_{\vec{r}}\cos(3\theta_{\vec{r}})$ showing the three-state Potts line $T_c(h_3)$. Path L in (a) maps to the eponymous path in (b).

three-sublattice ordered systems, it fails to account for the existence of $\mathcal{M}$. This underscores the importance of treating the uniform magnetization mode on the same footing as the three-sublattice order parameter.

I obtain numerical estimates of multicritical exponents and argue that such multicritical melting may be experimentally accessible in artificial kagome-ice systems if the strengths of nearest and next-nearest exchange interactions can be increased relative to the long-range dipolar interactions. Additionally, for $\eta(T) \in (\frac{1}{9}, \frac{2}{9})$ in the power-law ordered phase associated with two-step melting, I show that the *uniform susceptibility* to a small easy-axis field B diverges as $\chi(B) \sim |B|^{-[(4-18\eta)/(4-9\eta)]}$. I also argue that this easy-to-measure thermodynamic signature is of potential experimental relevance in the context of three-sublattice ordering of nearly half-filled monolayers of adsorbed gases on triangular substrates, and in the context of experimental realizations of three-sublattice order in $S = 1$ Heisenberg antiferromagnets with strong single-ion anisotropy on the triangular lattice.

Order parameters and coarse-graining.—I use the convention of Fig. 1 for labeling the sites (unit cells) $\vec{R} = m\hat{e}_x + n\hat{e}_y$ of the triangular (kagome) lattice and for labeling the three basis sites $\alpha = 0, 1, 2$ in each unit cell of the kagome lattice. With this convention, the complex three-sublattice order parameter $\psi \equiv |\psi|e^{i\theta}$ and the ferromagnetic order parameter M^z are defined as $\psi = -\sum_{\vec{R}} e^{i(2\pi/3)(m+n)} S^z_{\vec{R}}$ and $M^z = \sum_{\vec{R}} S^z_{\vec{R}}$ on the triangular lattice, while $\psi = -\sum_{\vec{R},\alpha} e^{i(2\pi/3)(m+n-\alpha)} S^z_{\vec{R},\alpha}$ and $M^z = \sum_{\vec{R},\alpha} S^z_{\vec{R},\alpha}$ on the kagome lattice. Our coarse-grained description will be written in terms of an effective Hamiltonian defined on a lattice whose sites $\vec{r}$ represent clusters of spins of the original triangular or kagome magnet. In this description, each cluster is characterized by an Ising variable $\tau_{\vec{r}} = \pm 1$ representing the direction of the local easy-axis magnetization $M^z_{\rm cluster}$ and by an angle $\theta_{\vec{r}}$ that represents the phase of the local three-sublattice order parameter $\psi_{\rm cluster}$. Comparison with long-wavelength properties of specific microscopic models is facilitated by choosing clusters that themselves form a coarse-grained triangular lattice, since this preserves the symmetries of the underlying triangular Bravais lattice in both triangular and kagome lattice systems.

Ginzburg-Landau theory.—Let us begin by summarizing in this language the standard Ginzburg-Landau theory for three-sublattice ordering [36–38]: transformation properties of ψ under global spin-flip and lattice symmetry operations fix the form of the effective Hamiltonian H_{xy} for $\theta_{\vec{r}}$. Leaving out certain chiral perturbations [45–47] that are not expected to be relevant [48] for the transitions of the lattice magnets studied here, H_{xy} may be written as

$$H_{xy} = -J_{xy}\sum_{\langle\vec{r}\vec{r}'\rangle}\cos(\theta_{\vec{r}} - \theta_{\vec{r}'}) - h_6\sum_{\vec{r}}\cos(6\theta_{\vec{r}}), \quad (1)$$

where $\langle\vec{r}\vec{r}'\rangle$ are nearest-neighbor links of our coarse-grained triangular lattice. The effective stiffness $J_{xy} > 0$ (encoding the energetic preference for three-sublattice order) and the sixfold anisotropy h_6, whose sign selects between ferrimagnetic three-sublattice order (with $\theta_m = 2\pi m/6$) and antiferromagnetic three-sublattice order [$\theta_m = (2m+1)\pi/6$], are both set by quantum fluctuations and subdominant further-neighbor couplings in the microscopic Hamiltonian. In this approach, the relative values of J_{xy} and its higher harmonics $J^{(p)}_{xy}$ [coefficients of $-\cos(p\theta_{\vec{r}} - p\theta_{\vec{r}'})$ for $p = 2, 3$] determine the nature of the melting process. These higher harmonics are omitted from H_{xy} displayed above since they are not crucial for our subsequent discussion.

New effective Hamiltonian.—Next, I note that this standard Ginzburg-Landau description does not take into account the uniform magnetization mode whose fluctuations are coupled in a crucial way to fluctuations of the

three-sublattice order parameter. This key observation leads me to a new coarse-grained effective model:

$$H_{\rm eff} = H_{xy} + H_{\rm Ising} - J_{\theta\tau}\sum_{\vec{r}} \tau_{\vec{r}} \cos(3\theta_{\vec{r}}),$$
$$\text{where } H_{\rm Ising} = -J_{\rm Ising}\sum_{\langle \vec{r}\vec{r}'\rangle} \tau_{\vec{r}}\tau_{\vec{r}'} - h\sum_{\vec{r}} \tau_{\vec{r}}, \quad (2)$$

with $h \propto B$. To understand the rationale for the form of this effective Hamiltonian, it is useful to first note that $H_{\rm eff}$ has the same $S_3 \times Z_2$ symmetry as H_{xy} and reduces, in the double limit $h_6, J_{\theta\tau} \to \infty$, to a generalized six-state clock model studied earlier [40,41]. However, the space of states at each site of $H_{\rm eff}$ is enlarged by the presence of $\tau_{\vec{r}}$ to correctly account for the fact that the direction of $M^z_{\rm cluster}$ is correlated with the phase of $\psi_{\rm cluster}$ but not completely tied to it. The microscopic origin of various terms can now be understood as follows: $J_{\rm Ising} > 0$ encodes the effect of subleading ferromagnetic interactions of the microscopic magnet, which tend to favor ferrimagnetic three-sublattice order. If $h_6 > 0$, it is likely to be accompanied by a sizeable positive value of $J_{\rm Ising}$ in $H_{\rm eff}$ (since ferrimagnetic three-sublattice order corresponds to $h_6 > 0$ in H_{xy}). Conversely, negative h_6, favored by quantum fluctuations in some examples [35], is likely to be accompanied by negligibly small $J_{\rm Ising}$. The coupling $J_{\theta\tau} > 0$ correctly captures the fact that the values $\theta = 0, 2\pi/3, 4\pi/3$ $(\pi/3, \pi, 5\pi/3)$, characteristic of ferrimagnetic three-sublattice order, are associated with a positive (negative) easy-axis magnetization, while the phase choices $\theta = (2m+1)\pi/6$, characteristic of antiferromagnetic three-sublattice order, are not associated with any net easy-axis magnetization (Fig. 1).

Phase diagram of $H_{\rm eff}$.—To deduce the structure of the $h = 0$ phase diagram of $H_{\rm eff}$ [Fig. 2(a)] in the $T - J_{\rm Ising}$ plane (with $J_{xy} = 1$) for fixed $\mathcal{O}(1)$ values of $J_{\theta\tau}$ and h_6, I start with the known phase diagrams of H_{xy} and $H_{\rm Ising}$ and analyze the effects of a nonzero $J_{\theta\tau}$. To this end, recall that $H_{\rm Ising}$ develops long-range order in τ for $T < T_\tau$, with long-distance properties of the critical point at T_τ described by a fixed-point free-energy functional $F_{1/2} = \int d^2x \mathcal{F}_{1/2}$ with central charge $c = 1/2$. Similarly, H_{xy} develops sixfold symmetry-breaking long-range order in θ for $T < T_{\theta 1}$, which melts via an intermediate phase with power-law correlations: $\langle e^{i(\theta(\vec{r})-\theta(0))}\rangle \sim 1/|\vec{r}|^{\eta(T)}$ with $\eta(T) \in (\frac{1}{9}, \frac{1}{4})$ for temperatures $T \in (T_{\theta 1}, T_{\theta 2})$ [42,43,49]. Long-wavelength properties of this power-law ordered phase are controlled, in renormalization group language, by a $c = 1$ line of fixed points [39], with effective free energy $F_{\rm KT} = \int d^2r \mathcal{F}_{\rm KT}$, where

$$\mathcal{F}_{\rm KT}/T = \frac{1}{4\pi g}(\nabla\theta)^2, \quad (3)$$

with $g(T) \in (\frac{1}{9}, \frac{1}{4})$ corresponding to $T \in (T_{\theta 1}, T_{\theta 2})$. This fixed line has power-law correlations $\langle e^{i(\theta(\vec{r})-\theta(0))}\rangle \sim 1/r^{\eta(g)}$ with $\eta(g) = g$, which render the sixfold symmetry-breaking perturbation $h_6 \cos(6\theta_{\vec{r}})$ irrelevant for $g > 1/9$ and vortices in θ irrelevant for $g < 1/4$ [39]. However, the threefold symmetric perturbation $h_3 \cos(3\theta_{\vec{r}})$ is relevant everywhere on this fixed line [39], implying that long-range order sets in at infinitesimal h_3 when $T < T_{\theta 2}$. In contrast, for fixed $T > T_{\theta 2}$, long-range order sets in via a three-state Potts transition [39] [Fig. 2(b)] only when a threshold $h_{3c}(T)$ is crossed; this defines a three-state Potts critical line $T_c(h_3)$ in the (T, h_3) phase diagram of H_{xy} [Fig. 2(b)]. Therefore, our analysis splits naturally into two cases, $T_\tau \lesssim T_{\theta 2}$ and $T_\tau \gtrsim T_{\theta 2}$, and relies crucially on the observation that long-range order of θ in H_{xy} leads to an external magnetic field of effective strength $h_{\rm eff} \equiv J_{\theta\tau}\langle\cos(3\theta)\rangle$ acting on τ in $H_{\rm Ising}$, while long-range order of τ in $H_{\rm Ising}$ perturbs H_{xy} by a threefold symmetric term $-\sum_{\vec{r}} h_{3\rm eff}\cos(3\theta_{\vec{r}})$ with $h_{3\rm eff} \equiv J_{\theta\tau}\langle\tau\rangle$.

$T_\tau \lesssim T_{\theta 2}$.—If $H_{\rm Ising}$ is in a short-range correlated paramagnetic phase in the entire temperature range $(T_{\theta 1}, T_{\theta 2})$, i.e., if $T_\tau \lesssim T_{\theta 1}$, a nonzero $J_{\theta\tau}$ only renormalizes the value of $g(T)$ that controls the power-law correlators of θ in this regime, and when the temperature is lowered below $T_{\theta 1}$, long-range order of θ in H_{xy} gives rise to an effective field $h_{\rm eff} \equiv J_{\theta\tau}\langle\cos(3\theta)\rangle$ in $H_{\rm Ising}$, converting the Ising transition at T_τ to a smooth crossover. On the other hand, if $T_{\theta 1} \lesssim T_\tau$, long-range order of τ below T_τ leads to a *threefold* symmetric perturbation $h_{3\rm eff}$ of H_{xy}, which immediately causes H_{xy} to develop long-range order in θ [Fig. 2(b)].

Thus, when $T_\tau \lesssim T_{\theta 2}$, $H_{\rm eff}$ is expected to display a sixfold symmetry-breaking long-range ordered state for $T < T_{c1}$, which undergoes a two-step melting transition via an intermediate power-law ordered phase [corresponding to $T \in (T_{c1}, T_{c2})$] with an exponent $\eta(T)$ that increases from $\eta(T_{c1}) = \frac{1}{9}$ to $\eta(T_{c2}) = \frac{1}{4}$. The value of T_{c1} is set (with deviations of order $J_{\theta\tau}$) by the larger of $T_{\theta 1}$ and T_τ, while that of T_{c2} is approximately set by $T_{\theta 2}$.

Power-law ordered phase.—Long-wavelength properties of $H_{\rm eff}$ in this power-law ordered intermediate phase can be described quite generally (for either sign of h_6) by an effective free-energy density

$$\mathcal{F}_{\tau\rm KT}/T = \mathcal{F}_{\rm KT}/T - c_{\theta\tau}\tau_{\vec{r}}\cos(3\theta_{\vec{r}}). \quad (4)$$

Although a nonzero $c_{\theta\tau}$ leads, upon tracing over τ, to the sixfold term $\cos(6\theta_{\vec{r}})$, which is irrelevant all along the fixed line parametrized by $c_{\theta\tau} = 0$ and $g(T) \in (\frac{1}{9}, \frac{1}{4})$ [as in Eq. (3)], I choose to retain a bare $c_{\tau\theta} \neq 0$ explicitly in Eq. (4) since this "dangerously irrelevant" coupling controls the long-distance correlations of $\tau_{\vec{r}}$ along this fixed line. Indeed, the nonzero value of $c_{\theta\tau}$ in $\mathcal{F}_{\tau\rm KT}$ causes $\tau_{\vec{r}}$ to inherit the power-law correlations of $\cos(3\theta_{\vec{r}})$ for all $T \in (T_{c1}, T_{c2})$: $\langle\tau_{\vec{r}}\tau_0\rangle \sim \langle e^{3i(\theta_{\vec{r}}-\theta_0)}\rangle \sim 1/r^{9g(T)}$. Ferromagnetic couplings between the Ising spins are not explicitly included in $\mathcal{F}_{\tau\rm KT}/T$ since the Ising bond energy $E_{\langle\vec{r}_1\vec{r}_2\rangle} \equiv \tau_{\vec{r}_1}\tau_{\vec{r}_2}$ has rapidly decaying correlations

$\langle E_{\langle \vec{r}_1 \vec{r}_2 \rangle} E_{\langle \vec{r}_3 \vec{r}_4 \rangle} \rangle \sim 1/r^{36g}$ (r is the distance between bonds $\langle \vec{r}_1 \vec{r}_2 \rangle$ and $\langle \vec{r}_3 \vec{r}_4 \rangle$) that render these couplings irrelevant along this fixed line. Just below $g = 1/9$ (i.e., for $T < T_{c1}$), the ferromagnetic couplings between the $\tau_{\vec{r}}$ and the sixfold anisotropy term $\cos(6\theta_{\vec{r}})$ both become relevant. This signals the onset of sixfold symmetry-breaking long-range order in $H_{\rm eff}$.

Singular susceptibility.—For $\eta(T) < \frac{2}{9}$ in this power-law ordered intermediate phase of $H_{\rm eff}$, the foregoing implies that power-law correlations of τ decay slowly enough that they lead to a *divergent* contribution $\chi_{\rm sing} \sim L^{2-9\eta}$ to the finite-size susceptibility χ_L of an $L \times L$ system at $h = 0$. This implies $\chi_L(T) = \chi_{\rm reg}(T) + b(T) L^{2-9\eta(T)}$ for $\eta(T) \in (\frac{1}{9}, \frac{2}{9})$. When an external field h is turned on in this regime, it perturbs $\mathcal{F}_{\tau \rm KT}$ with a threefold symmetric perturbation $J_{\theta\tau} \chi_{\rm reg} h \cos(3\theta_{\vec{r}})$. This drives $H_{\rm eff}$ to a long-range-ordered state with correlation length $\xi(h) \sim |h|^{-1/\lambda_3(g)}$, where $\lambda_3(g) = 2 - 9g/2$. Beyond this correlation-length scale, $H_{\rm eff}$ resembles a three-state Potts model in its ordered state [39]. Therefore, for small nonzero h, $\chi_{\rm sing}$ will be cut off at length scales of order this correlation length $\xi(h)$, giving rise to a thermodynamic susceptibility that scales as $[\xi(h)]^{2-9\eta(T)}$ at small h. For the thermodynamic easy-axis susceptibility of the microscopic easy-axis antiferromagnet, the foregoing analysis thus predicts

$$\chi(B) \sim |B|^{-\{[4-18\eta(T)]/[4-9\eta(T)]\}} \tag{5}$$

at small $|B|$ for $\eta(T) \in (\frac{1}{9}, \frac{2}{9})$. This prediction identifies an experimentally useful signature of two-step melting of either type (ferrimagnetic or antiferromagnetic) of three-sublattice order in triangular and kagome lattice easy-axis magnets. In particular, it applies to the $S = 1$ triangular lattice Heisenberg antiferromagnet with strong single-ion anisotropy [29,33] and to the triangular lattice Ising antiferromagnet with further-neighbor couplings [12]. It would therefore be interesting to identify quasi-two-dimensional magnets in the $Ca_3Co_2O_6$ family [50,51] (with an angular momentum $J = 1$ ion at one Co site and a nonmagnetic ion at the other) which could provide experimental realizations of the former. It would also be interesting to identify new combinations of substrate and adsorbate for which monolayer densities closer to half-filling (than hitherto achievable [5–11]), corresponding to $B \ll 1$ in the latter, could be reached for monolayers of adsorbed gases on triangular substrates.

$T_\tau \gtrsim T_{\theta 2}$.—In this case, $H_{\rm eff}$ develops long-range order in τ via a transition in the Ising universality class at T_{cI} [Fig. 2(a)], with the value of T_{cI} set by T_τ (with deviations of order $J_{\theta\tau}$). For $T < T_{cI}$, the spontaneous magnetization $\langle \tau \rangle$ perturbs H_{xy} with the threefold field $h_{3\rm eff}$. Lowering the temperature below T_{cI} along path L in the phase diagram of $H_{\rm eff}$ [Fig. 2(a)] therefore corresponds to moving along the eponymous path L in the known [39] phase diagram of $H_{xy} - h_3 \sum_{\vec{r}} \cos(3\theta_{\vec{r}})$ [Fig. 2(b)]. This key observation immediately leads to two conclusions: First, $H_{\rm eff}$ must develop long-range order in θ at a *lower* temperature $T_{cP} < T_{cI}$ via a three-state Potts transition [Fig. 2(a)]. Second, these Ising and three-state Potts transition lines (T_{cI} and T_{cP}) must meet the phase boundaries of the power-law ordered phase (T_{c2} and T_{c1}) at a single multicritical point $\mathcal{M}$ [Fig. 2(a)].

Multicritical point.—The fixed point theory $F_{\mathcal{M}}$ that controls long-distance properties of $\mathcal{M}$ can be reached from the $c = 3/2$ theory $F_{1/2} + F_{\rm KT}$ (with $g = 1/4$) by turning on the relevant perturbation $J_{\theta\tau}$. The c theorem [44] therefore predicts that the central charge of $F_{\mathcal{M}}$ obeys $c_{\mathcal{M}} < \frac{3}{2}$. Since $F_{\mathcal{M}}$ must have a relevant direction leading from it to the $c = 1$ theory $F_{\tau \rm KT}$, the c theorem also predicts $c_{\mathcal{M}} > 1$. At $\mathcal{M}$, the correlation functions $C_\tau(\vec{r}) = \langle \tau(\vec{r}) \tau(0) \rangle$ and $C_{p\theta}(\vec{r}) = \langle e^{ip\theta(\vec{r})} e^{-ip\theta(0)} \rangle$ ($p = 1, 2, 3$) are expected to have the long-distance forms: $C_\tau(\vec{r}) = 1/r^{\eta_\tau}$, $C_{p\theta}(\vec{r}) \sim 1/r^{\eta_{p\theta}}$ (with $\eta_{3\theta} = \eta_\tau$ on symmetry grounds). Setting $J_{xy} = h_6 = 1.0$, $J_{\theta\tau} = 0.25$, and parametrizing $J_{\rm Ising} = f_{xy} T_{\theta_1}/T_\tau$ and $T = f_I f_{xy} T_{\theta 1}$, with $T_{\theta 1} = 1.04$ and $T_\tau = 3.6409$, I have performed extensive Monte Carlo simulations of $H_{\rm eff}$ to locate and study $\mathcal{M}$. Figure 3 displays power-law fits for the L dependence of $C_\tau(\vec{r}_L)$ and $C_{p\theta}(\vec{r}_L)$ at separation $\vec{r}_L = (L/3)\hat{e}_x$ on periodic $L \times L$ triangular lattices at my best estimate for $\mathcal{M}$, given by $[f_{xy}^{\mathcal{M}}, f_I^{\mathcal{M}}] \approx [1.5570(8), 1.0061(5)]$. Such fits yield the following estimates for multicritical exponents:

$$\eta_{3\theta} = \eta_\tau \approx 0.201(20); \qquad \eta_\theta \approx 0.258(5); \qquad \eta_{2\theta} \approx 0.353(6). \tag{6}$$

This set of exponents is clearly different from the well-known exponents in the power-law ordered phase

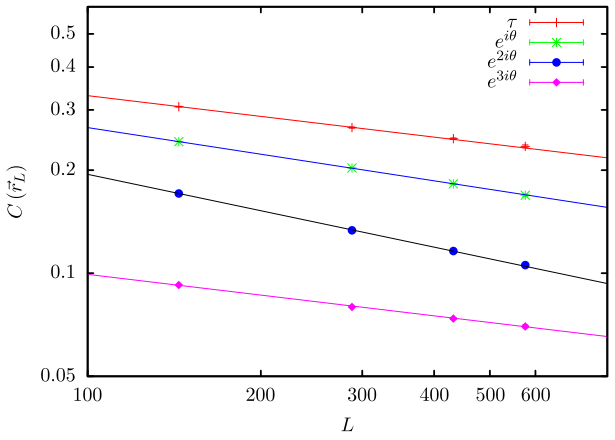

FIG. 3 (color online). L dependence of $C_\tau(\vec{r}_L)$ and $C_{p\theta}(\vec{r}_L)$ ($p = 1, 2, 3$) at separation $\vec{r}_L = \hat{e}_x(L/3)$ on periodic $L \times L$ triangular lattices, evaluated at the estimated location $[f_{xy}^{\mathcal{M}}, f_I^{\mathcal{M}}] = [1.5570, 1.0061]$ of the multicritical point of $H_{\rm eff}$ with $J_{xy} = h_6 = 1.0$, $J_{\theta\tau} = 0.25$ (notation as in text). Lines denote fits to $1/L^{\eta_\tau}$ and $1/L^{\eta_{p\theta}}$, respectively, using $\eta_{3\theta} = \eta_\tau = 0.201$, $\eta_\theta = 0.258$, and $\eta_{2\theta} = 0.353$. $C_{2\theta}$ ($C_{3\theta}$) is rescaled by a factor of 7 (factor of 10) for clarity.

$[\eta_{p\theta} = p^2\eta(T)]$ or on the three-state Potts line ($\eta_{2\theta} = \eta_\theta = 4/15$) or the Ising line ($\eta_{3\theta} = \eta_\tau = 1/4$).

I close by noting an intriguing possibility: since three-sublattice order melts via a three-state Potts transition in the kagome Ising antiferromagnet with dipolar interactions [19–21], while the analogous short-ranged model with nearest- and next-nearest-neighbor exchange couplings exhibits two-step melting behavior [21,23,24], it appears likely that such multicritical melting could be seen in artificial kagome-ice systems if the strength of the first- and second-neighbor exchange interactions could be increased relative to the long-range dipolar couplings (whose values are fixed by magnetostatics).

I thank F. Alet, M. Barma, D. Dhar, and R. Kaul for useful comments on an earlier draft, G. Mandal, S. Minwalla, and S. Trivedi for a survey of well-known $c > 1$ conformal field theories, and R. G. Ghanshyam for help with figures. The numerical work described here was made possible by the computational resources of the Department of Theoretical Physics of the TIFR. A major part of the analysis reported here was completed while participating in the Program on Frustrated Magnetism and Quantum Spin Liquids at KITP Santa Barbara, where this work was informed by useful discussions with T. Grover and a review of the artificial kagome-ice literature by R. Moessner. Participation in this program was made possible by partial support from National Science Foundation Grant No. NSF PHY11-25915.

[1] R. Moessner and A. P. Ramirez, Phys. Today **59**, No. 2, 24 (2006).
[2] L. Balents, Nature (London) **464**, 199 (2010).
[3] A. Sen, F. Wang, K. Damle, and R. Moessner, Phys. Rev. Lett. **102**, 227001 (2009).
[4] A. Sen, K. Damle, and A. Vishwanath, Phys. Rev. Lett. **100**, 097202 (2008).
[5] M. Bretz, J. G. Dash, D. C. Hickernell, E. O. McLean, and O. E. Vilches, Phys. Rev. A **8**, 1589 (1973).
[6] M. Bretz, Phys. Rev. Lett. **38**, 501 (1977).
[7] P. M. Horn, R. J. Birgeneau, P. Heiney, and E. M. Hammonds, Phys. Rev. Lett. **41**, 961 (1978).
[8] O. E. Vilches, Annu. Rev. Phys. Chem. **31**, 463 (1980).
[9] R. M. Suter, N. J. Colella, and R. Gangwar, Phys. Rev. B **31**, 627(R) (1985).
[10] Y. P. Feng and M. H. W. Chan, Phys. Rev. Lett. **64**, 2148 (1990).
[11] H. Wiechert, Physica (Amsterdam) **169B**, 144 (1991).
[12] D. P. Landau, Phys. Rev. B **27**, 5604 (1983).
[13] G. H. Wannier, Phys. Rev. **79**, 357 (1950).
[14] J. Stephenson, J. Math. Phys. **5**, 1009 (1964).
[15] M. Tanaka, E. Saitoh, H. Miyajima, T. Yamaoka, and Y. Iye, Phys. Rev. B **73**, 052411 (2006).
[16] Y. Qi, T. Brintlinger, and J. Cumings, Phys. Rev. B **77**, 094418 (2008).
[17] S. Ladak, D. E. Read, G. K. Perkins, L. F. Cohen, and W. R. Branford, Nat. Phys. **6**, 359 (2010).
[18] S. Ladak, D. E. Read, W. R. Branford, and L. F. Cohen, New J. Phys. **13**, 063032 (2011).
[19] G. Moller and R. Moessner, Phys. Rev. B **80**, 140409(R) (2009).
[20] G.-W. Chern, P. Mellado, and O. Tchernyshyov, Phys. Rev. Lett. **106**, 207202 (2011).
[21] G.-W. Chern and O. Tchernyshyov, Phil. Trans. R. Soc. A **370**, 5718 (2012).
[22] K. Kano and S. Naya, Prog. Theor. Phys. **10**, 158 (1953).
[23] M. Wolf and K. D. Schotte, J. Phys. A **21**, 2195 (1988).
[24] T. Takagi and M. Mekata, J. Phys. Soc. Jpn. **62**, 3943 (1993).
[25] A. S. Wills, R. Ballou, and C. Lacroix, Phys. Rev. B **66**, 144407 (2002).
[26] B. Nienhuis, H. J. Hilhorst, and H. W. J. Blote, J. Phys. A **17**, 3559 (1984).
[27] C. Zeng and C. L. Henley, Phys. Rev. B **55**, 14935 (1997).
[28] R. G. Melko, A. Paramekanti, A. A. Burkov, A. Vishwanath, D. N. Sheng, and L. Balents, Phys. Rev. Lett. **95**, 127207 (2005).
[29] D. Heidarian and K. Damle, Phys. Rev. Lett. **95**, 127206 (2005).
[30] S. Wessel and M. Troyer, Phys. Rev. Lett. **95**, 127205 (2005).
[31] G. Murthy, D. Arovas, and A. Auerbach, Phys. Rev. B **55**, 3104 (1997).
[32] M. Boninsegni and N. Prokof'ev, Phys. Rev. Lett. **95**, 237204 (2005).
[33] K. Damle and T. Senthil, Phys. Rev. Lett. **97**, 067202 (2006).
[34] A. Sen, P. Dutt, K. Damle, and R. Moessner, Phys. Rev. Lett. **100**, 147204 (2008).
[35] S. V. Isakov and R. Moessner, Phys. Rev. B **68**, 104409 (2003).
[36] E. Domany, M. Schick, J. S. Walker, and R. B. Griffiths, Phys. Rev. B **18**, 2209 (1978).
[37] E. Domany and M. Schick, Phys. Rev. B **20**, 3828 (1979).
[38] S. Alexander, Phys. Lett. **54A**, 353 (1975).
[39] J. V. José, L. P. Kadanoff, S. Kirkpatrick, and D. R. Nelson, Phys. Rev. B **16**, 1217 (1977).
[40] J. L. Cardy, J. Phys. A **13**, 1507 (1980).
[41] P. Dorey, P. Provero, R. Tateo, and S. Vinti, J. Phys. A **32**, L151 (1999).
[42] J. Tobochnik, Phys. Rev. B **26**, 6201 (1982).
[43] M. S. S. Challa and D. P. Landau, Phys. Rev. B **33**, 437 (1986).
[44] J. Cardy, in *Scaling and Renormalization in Statistical Physics*, Cambridge Lecture Notes in Physics, edited by P. Goddard and J. Yeomans (Cambridge University Press, Cambridge, England, 1996).
[45] D. A. Huse and M. E. Fisher, Phys. Rev. B **29**, 239 (1984).
[46] D. A. Huse and M. E. Fisher, Phys. Rev. Lett. **49**, 793 (1982).
[47] M. Kardar and A. N. Berker, Phys. Rev. Lett. **48**, 1552 (1982).
[48] D. A. Huse, Phys. Rev. B **29**, 5031 (1984).
[49] E. Rastelli, S. Regina, and A. Tassi, Phys. Rev. B **69**, 174407 (2004).
[50] J. A. M. Paddison, S. Agrestini, M. R. Lees, C. L. Fleck, P. P. Deen, A. L. Goodwin, J. R. Stewart, and O. A. Petrenko, Phys. Rev. B **90**, 014411 (2014).
[51] K. E. Stitzer, J. Darriet, and H.-C. zur Loye, Curr. Opin. Solid State Mater. Sci. **5**, 535 (2001).